Food Chemistry 204 (2016) 218–226

Contents lists available at ScienceDirect

Food Chemistry

journal homepage: www.elsevier.com/locate/foodchem

Certain (−)-epigallocatechin-3-gallate (EGCG) auto-oxidation products (EAOPs) retain the cytotoxic activities of EGCG

Yaqing Wei [a,1], Pingping Chen [a,1], Tiejun Ling [a,b,1], Yijun Wang [a], Ruixia Dong [a], Chen Zhang [c], Longjie Zhang [a], Manman Han [a], Dongxu Wang [a], Xiaochun Wan [a], Jinsong Zhang [a,*]

[a] State Key Laboratory of Tea Plant Biology and Utilization, School of Tea and Food Science, Anhui Agricultural University, Anhui 230036, China
[b] Collaborative Mass Spectrometry Innovation Center, Skaggs School of Pharmacy and Pharmaceutical Sciences, University of California, San Diego, La Jolla, CA 92093, United States
[c] Department of Stomatology, Anhui Medical College, Anhui 230000, China

ARTICLE INFO

Article history:
Received 16 July 2015
Received in revised form 5 February 2016
Accepted 21 February 2016
Available online 23 February 2016

Keywords:
EGCG
Auto-oxidation
Cytotoxic activity
Sulfhydryl group
Hydrogen peroxide

ABSTRACT

(−)-Epigallocatechin-3-gallate (EGCG) from green tea has anti-cancer effect. The cytotoxic actions of EGCG are associated with its auto-oxidation, leading to the production of hydrogen peroxide and formation of numerous EGCG auto-oxidation products (EAOPs), the structures and bioactivities of them remain largely unclear. In the present study, we compared several fundamental properties of EGCG and EAOPs, which were prepared using 5 mg/mL EGCG dissolved in 200 mM phosphate buffered saline (pH 8.0 at 37 °C) and normal oxygen partial pressure for different periods of time. Despite the complete disappearance of EGCG after the 4-h auto-oxidation, 4-h EAOPs gained an enhanced capacity to deplete cysteine thiol groups, and retained the cytotoxic effects of EGCG as well as the capacity to produce hydrogen peroxide and inhibit thioredoxin reductase, a putative target for cancer prevention and treatment. The results indicate that certain EAOPs possess equivalent cytotoxic activities to EGCG, while exhibiting simultaneously enhanced capacity for cysteine depletion. These results imply that EGCG and EAOPs formed extracellularly function in concert to exhibit cytotoxic effects, which previously have been ascribed to EGCG alone.

1. Introduction

Tea made from the leaves of the plant *Camellia sinensis* is the most widely consumed beverage second only to water. It has been used since ancient times for medicinal purposes. One of the major health-giving ingredient of green tea is catechins, including (−)-epicatechin (EC), (−)-epigallocatechin (EGC), (−)-epicatechin-3-gallate (ECG) and (−)-epigallocatechin-3-gallate (EGCG). In some types of green tea, the catechin content can be as high as 30–40% of the dry weight. Among the various catechins, EGCG is most abundant (nearly half of the total) and exhibits the highest biological activities in general. On the basis of catechin oxidation during processing, tea is classified into two major types: green tea and black tea. Catechin oxidation is deliberately inhibited via high-temperature inactivation of polyphenol oxidases in green tea which is mostly popular in China and Japan, whereas the oxidation is intentionally promoted to form dimerized theaflavins and polymerized thearubigins through optimizing the conditions favouring the interaction between catechins and polyphenol oxidases in black tea consumed worldwide (Khan & Mukhtar, 2013; Sang, Lambert, Ho, & Yang, 2011; Zhang, Wei, & Zhang, 2014).

Over the past two decades, tea has been extensively studied for its health-beneficial effects, including prevention of cancer, cardiovascular and neurodegenerative diseases, metabolic syndrome alleviation, and body weight control (Yang & Hong, 2013). Cancer prevention using green tea or catechins is the most studied field. Some, although not all, epidemiologic studies have established a relationship between green tea consumption, particularly at high intake levels, and reduced risks of certain types of cancer (Yuan, 2013). Numerous animal experiments have convincingly shown that EGCG exerts an anti-cancer effect at relatively high but tolerable doses (Siddiqui et al., 2009; Wang, Taylor, Wang, Wan, & Zhang, 2012). Similarly, many cell culture studies have demonstrated that EGCG at the dose unable to cause perceived toxicity in normal cells triggers pronounced cytotoxicity in tissue paired cancer cells (Kumazoe et al., 2013; Shammas et al., 2006).

The highly reactive attributes of EGCG are conferred by its chemical structure. In the B-ring and D-ring of EGCG, the vicinal trihydroxy group participates in electron delocalization for quenching free radicals or scavenging reactive oxygen species

* Corresponding author.
E-mail address: zjs@ahau.edu.cn (J. Zhang).
[1] Contributed equally.

http://dx.doi.org/10.1016/j.foodchem.2016.02.134
0308-8146/

(ROS), such as superoxide anions, hydroxyl radicals, singlet oxygen, peroxyl radicals, nitric oxide, nitrogen dioxide and peroxynitrite (Sang et al., 2011). The vicinal trihydroxy group in the B-ring is the principal site responsible for antioxidant reactions, which are further enhanced by the vicinal trihydroxy group in the D-ring (Sang et al., 2011; Severino et al., 2009). On the other hand, these highly active trihydroxys also render EGCG susceptible to oxidation in air under neutral or especially, alkaline pH (Sang et al., 2011; Severino et al., 2009). Auto-oxidation of EGCG generates ROS, with EGCG simultaneously transformed into numerous EGCG auto-oxidation products (EAOPs) (Sang et al., 2011; Severino et al., 2009). The auto-oxidation of EGCG also occurs under cell culture conditions. The half-life of EGCG was less than 30 min in McCoy's 5A culture media (Hong et al., 2002). To date, the bioactivities of EAOPs have not been elucidated in detail. Therefore, in the present study, we compared several fundamental biological properties of EGCG and EAOPs prepared using 5 mg/mL EGCG dissolved in 200 mM phosphate buffer solution (PBS), pH 8.0, at 37 °C and under normal oxygen partial pressure for 2, 4, 8, 16 and 32 h.

2. Materials and methods

2.1. Cells and chemicals

The human squamous carcinoma cell line Tca8113 was obtained from the Key Laboratory of Oral Biomedicine of Shanghai Jiaotong University (China). The murine colon carcinoma cell line CT26 was purchased from ATCC (ATCC® CRL-2638™). RPMI 1640 medium, fetal calf serum (FCS), trypsin and penicillin–streptomycin were products of HyClone (Logan, UT, USA). 3-(4,5-Dimethyl-2-thiazolyl)-2,5-diphenyltetrazolium bromide (MTT) was a product of Amresco LLC (Solon, OH, USA). Reduced nicotinamide adenine dinucleotide phosphate (NADPH), dimethylsulfoxide (DMSO), 5,5′-dithiobis (2-nitrobenzotic acid) (DTNB), thioredoxin reductase 1 (TrxR1) purified from rat liver, bovine serum albumin (BSA), 2′,7′-dichlorofluorescein diacetate (DCFH-DA), glutathione (GSH), L-cysteine hydrochloride (Cys), superoxide dismutase (SOD) and catalase (CAT) were purchased from Sigma (St. Louis, MO, USA). The hydrogen peroxide test kit was purchased from Beyotime (Nantong, P.R. China). EGCG (>99% purity) and gallic acid (GA) were products of Yibeijia Tea Technology, Inc. (Hangzhou, P.R. China). Other chemicals were of the highest grade available.

2.2. Preparation of EAOPs

EGCG was dissolved in 200 mM PBS (pH 8.0) at a concentration of 5 mg/mL, and was pipetted into 12 × 100 mm glass tubes (1 mL/tube). Auto-oxidation of EGCG was carried out at 37 °C for 0, 2, 4, 8, 16 and 32 hours. EGCG and the EAOPs were instantly stored at −20 °C.

2.3. Spectral analysis

EGCG and EAOPs were diluted to 100 μg/mL for spectral scanning at 200–550 nm or 1 mg/mL for spectral scanning at 350–700 nm using a U-3010 spectrophotometer (Hitachi Ltd., Tokyo, Japan).

2.4. HPLC assay

A Waters HPLC system equipped with a Waters 600 controller and the Waters 2489 UV/Visible detector was employed (Waters Instruments, Inc., Rochester, MN). Chromatographic separation was performed on a Gemini 5u C18 110A column, 250 × 4.60 mm (Phenomenex Inc., Torrance, CA). The mobile phase consisted of (A) deionized water with 0.15% acetic acid and (B) acetonitrile. The following gradient was used: 0 min at 85% A, a linear gradient to 77% A for 10 min, then a linear gradient to 71% A for 35 min before phase A was reduced to 0% within 1 min, held for 4 min, and returned to 85% A for 2 min. The column temperature was set at 30 °C. All the samples were diluted to 500 μg/mL and the injection volume was 5 μL. The elution rate was 0.8 mL/min, and the detection wavelength was set at 278 nm.

2.5. Ultra performance liquid chromatography–electrospray ionization mass spectrometric (UPLC–ESI-MS) and ultra liquid chromatography-tandem mass spectrometric (UPLC–MS/MS) analysis

UPLC–ESI–MS and UPLC–MS/MS analyses were performed on a micrOTOF-Q II system (Bruker). EAOPs were prepared in 200 mM Tris-HCl (pH 8.0) according to the above method. The sample of 2-h EAOPs (5 μL, 5 mg/mL) was diluted by 10-fold with water and applied to a Phenomenex column (Kinetex 1.7u C18 100A, 50 × 2.1 mm) with temperature maintained at 40 °C. The mobile phases A and B were 0.1% aqueous formic acid and acetonitrile, respectively. The gradient of solvent B was as follows: 0–1.34 min, from 5% to 10%; 1.34–7 min, from 10% to 29%; 7–7.5 min, from 29% to 100%; then kept at 100% to 8.4 min; 8.4–8.5 min, from 100% to 5%; then kept at 5% to 9 min. Solvent flow rate was 0.5 mL/min. The MS instrument was operated using an ESI source in positive ionization mode. The ion scan range was 100–3000 *m/z*. The dry gas was set to 9 L/min at 200 °C with a nebulization gas pressure of 2.0 bar. In the MS/MS experiments, the quadruple ion energy and the collision energy were adjusted to 4 and 8 eV, respectively. The data of UPLC–MS/MS were analyzed by Compass DataAnalysis software (Bruker Daltonics).

2.6. Cell culture and MTT assays

Tca8113 or CT26 cell lines were maintained in complete medium (RPMI-1640 medium supplemented with 10% (v/v) FCS, 100 U/mL penicillin and 100 μg/mL streptomycin) at 37 °C under 5% CO_2 and 95% air. Cells were transferred to 96-well culture plates at 10^4 cells/well for proliferation inhibition assays 24 h prior to each experiment. Tca8113 or CT26 cells were treated with EGCG or EAOPs in complete medium for 2 or 3 days, respectively. The medium was then removed and 200 μL RPMI-1640 medium containing 0.5 mg/mL MTT was added to each well. After incubation for 4 h, the medium was replaced with 150 μL DMSO, and the absorbance at 490 nm was measured.

2.7. Quantification of sulfhydryl group levels

The reaction of Cys/GSH and EGCG/EAOPs was maintained at 37 °C in 100 μL solution composed of EGCG/EAOPs, PBS (200 mM, pH 8.0) and 25 mM Cys/GSH. Sulfhydryl group levels were then measured using DTNB assays. Briefly, 2 μL of the reaction solution was added to 200 μL PBS (200 mM, pH 8.0) with 0.1 mg/mL DTNB and the absorbance at 412 nm was measured.

2.8. Measurement of ROS

EGCG or EAOPs were incubated in 200 μL PBS (200 mM, pH 8.0) with 100 μM DCFH-DA in a 96-well plate. Fluorescence intensity was measured using a plate reader (California, USA, Molecular Devices) at an excitation wavelength of 488 nm and an emission wavelength of 525 nm.

2.9. Determination of hydrogen peroxide concentrations

EGCG or EAOPs were incubated at 37 °C in 500 μL PBS (20 mM, pH 8.0), and the concentration of hydrogen peroxide was determined using a kit according to manufacturer's protocol. Briefly, 50 μL sample solution and 150 μL working solution were added to a 96-well plate and absorbance at 595 nm was measured after incubation for 30 min at 25 °C.

2.10. Determination of TrxR activity

The reaction of purified TrxR1 and EGCG or EAOPs was performed at 37 °C for 20 min in a 96-well plate containing 50 μL solution composed of EGCG/EAOPs, PBS (200 mM, pH 8.0), 1.5 μL purified TrxR1 and 300 μM NADPH. TrxR activity was then determined by adding 250 μL working solution (200 mM PBS, pH 8.0 containing 2 mg/mL DTNB, 0.2 mg/mL NADPH and 0.2 mg/mL BSA) and absorbance at 412 nm was measured (Wang, Sun, Tan, Wu, & Zhang, 2014).

2.11. Statistical analysis

Data are presented as the mean ± standard error of the mean (SEM). The differences between groups were examined by one way ANOVA *post hoc* Tukey's multiple comparison tests using GraphPad software (Prism, version 5, San Diego, CA, USA). A *P*-value of <0.05 was considered to indicate statistical significance.

3. Results

3.1. Characteristics of EGCG and EAOPs

EGCG at a concentration of 5 mg/mL in 200 mM PBS (pH 8.0) was maintained at 37 °C for 2, 4, 8, 16 and 32 h. The color (brown) intensity and visible absorption of EAOPs increased in a time-dependent manner (Fig. 1A and B). Two-hour EAOPs were separated by HPLC into at least nine peaks (Fig. 1C), suggesting that EAOPs consist of multiple components. However, many of the peaks seen in 2-h EAOPs were absent in 4-h EAOPs, indicating that EAOPs, like EGCG, are unstable (Fig. 1C). Along with the decrease of EGCG, GA, a component of EGCG, increased (Fig. 1C). Further experiments showed that EGCG oxidation ratio was inversely associated with its concentration (Fig. 1D).

3.2. Characterization of 2-h EAOPs using UPLC-ESI-MS and UPLC-MS/MS

A sample of 2-h EAOPs was specifically prepared in 200 mM Tris-HCl (pH 8.0) for UPLC–ESI-MS and UPLC–MS/MS analysis. The total ion chromatogram (TIC) of UPLC–ESI-MS was preliminary scanned and showed no more valuable information except the occurrence of EGCG and GCG in the sample (Fig. 2A, B, D and Supplementary Fig. S1, S2). On the other hand, EGCG is able to form theasinensin A and (or) theasinensin D, dimer quinone, or some other polyphenols in weak alkaline condition (Sang, Yang, Buckley, Ho, & Yang, 2007). Therefore, the specific molecular information of all possible structures was put into Compass DataAnalysis and investigated in the extracted ion chromatogram (EIC) mode. As a result, only 915.1624 ($M + H^+$), which is the quasi molecular weight of theasinensin A (or D) ($C_{44}H_{35}O_{22}^+$, Calcd: 915.1614), was found in the dataset (Fig. 2C). The identification of theasinensin A (or D) in the sample was supported by analysis of the MS/MS spectrum (Fig. 2E, F and Supplementary Fig. S3). In MS/MS spectrum of *m/z* 915.1624, several characteristic fragments due to loosing of gallic acid unit, i.e., *m/z* 745.1445, 575.1209 and 593.1280 were observed. In addition, the strong signal at *m/z* 139.0382, which was generated from RDA fission of pyran in theasinensin A (or D), also supported the identification (Menet, Sang, Yang, Ho, & Rosen, 2004). Therefore, theasinensin A (or D) was suggested as one of the main components in 2-h EAOPs despite the complex chemical features of EAOPs.

3.3. Anti-proliferative activities of EGCG and EAOPs

Ninety-six-well culture plates were seeded with human squamous carcinoma Tca8113 cells or murine colon carcinoma CT26 cells at a density of 10^4 cells per well. EGCG dose-dependently suppressed the proliferation of Tca8113 cells, with maximum inhibition observed at dose of 30 μg/mL (Fig. 3A); this dose was chosen to compare the anti-proliferative activities of EAOPs and EGCG. EGCG and EAOPs achieved equivalent anti-proliferative activities at the same dose, with a exception of 32-h EAOPs, the efficacy of which was significantly but only slightly less than that of EGCG (Fig. 3B). In the case of CT26 cells, based on the dose effect of EGCG (Fig. 3C), the comparison of EGCG and EAOPs in suppressing CT26 cell proliferation was carried out at a dose of 20 μg/mL. Similarly, we found that, with the exception of 32-h EAOPs, the anti-proliferative activity of EGCG and EAOPs remained identical (Fig. 3D).

In summary, extensive EGCG auto-oxidation tends to compromise the cytotoxic activity of EGCG, as typically observed for 32-h EAOPs. However, EAOPs derived from moderate EGCG auto-oxidation, for example, 4-h EAOPs wherein EGCG no longer existed, largely retain the cytotoxic activity of EGCG. Overall, EGCG auto-oxidation does not necessarily cause an obvious alteration in cytotoxic activity. The chemical properties of EGCG in terms of producing ROS and hydrogen peroxide, high affinity binding to enzymes and reaction with the sulfhydryl group of Cys residues have been extensively elucidated. Based on the preservation of cytotoxic activity after pronounced alterations in the chemical structure of EGCG observed in certain EAOPs, we afterwards investigated whether the chemical properties of EGCG are significantly influenced by its auto-oxidation.

3.4. Chemical properties of EGCG and EAOPs

EGCG undergoes auto-oxidation in air-saturated alkaline pH buffer. Oxygen obtains electron from EGCG, resulting in the formation of superoxide anions, which are eventually reduced; consequently hydrogen peroxide is accumulated. As shown in Fig. 4A, EGCG produced hydrogen peroxide in a time- and dose-dependent manner. The time-dependent feature of this reaction was more prominent at a dose of 20 μg/mL EGCG within 1 h; thus, we compared the capacities of EAOPs and EGCG at this dose and over a 1-h time frame (Fig. 4B). As expected, EGCG auto-oxidation led to a reduction in hydrogen peroxide production, with the exception of 2- or 4-h EAOPs, which retained the same capacity as EGCG.

As shown in Fig. 4C, EGCG produced ROS in a time- and dose-dependent manner within the concentration below 400 μg/mL, whereas high-dose of EGCG did not further generate ROS, due to oxygen deficiency in the reaction system. We thus compared the capacities of EAOPs and EGCG to produce ROS at a dose of 200 μg/mL to ensure the presence of sufficient oxygen. Unexpectedly, 16- and 32-h EAOPs, particularly the latter, produced more ROS than EGCG at many of the observed time-points (Fig. 4D); thus, it is tempting to conclude that EAOPs derived from extensive auto-oxidation of EGCG facilitate ROS production. The ROS generated from EGCG were shown to consist of superoxide anions and hydrogen peroxide based on the observation that CAT and SOD alone suppressed ROS production, while the combination of CAT

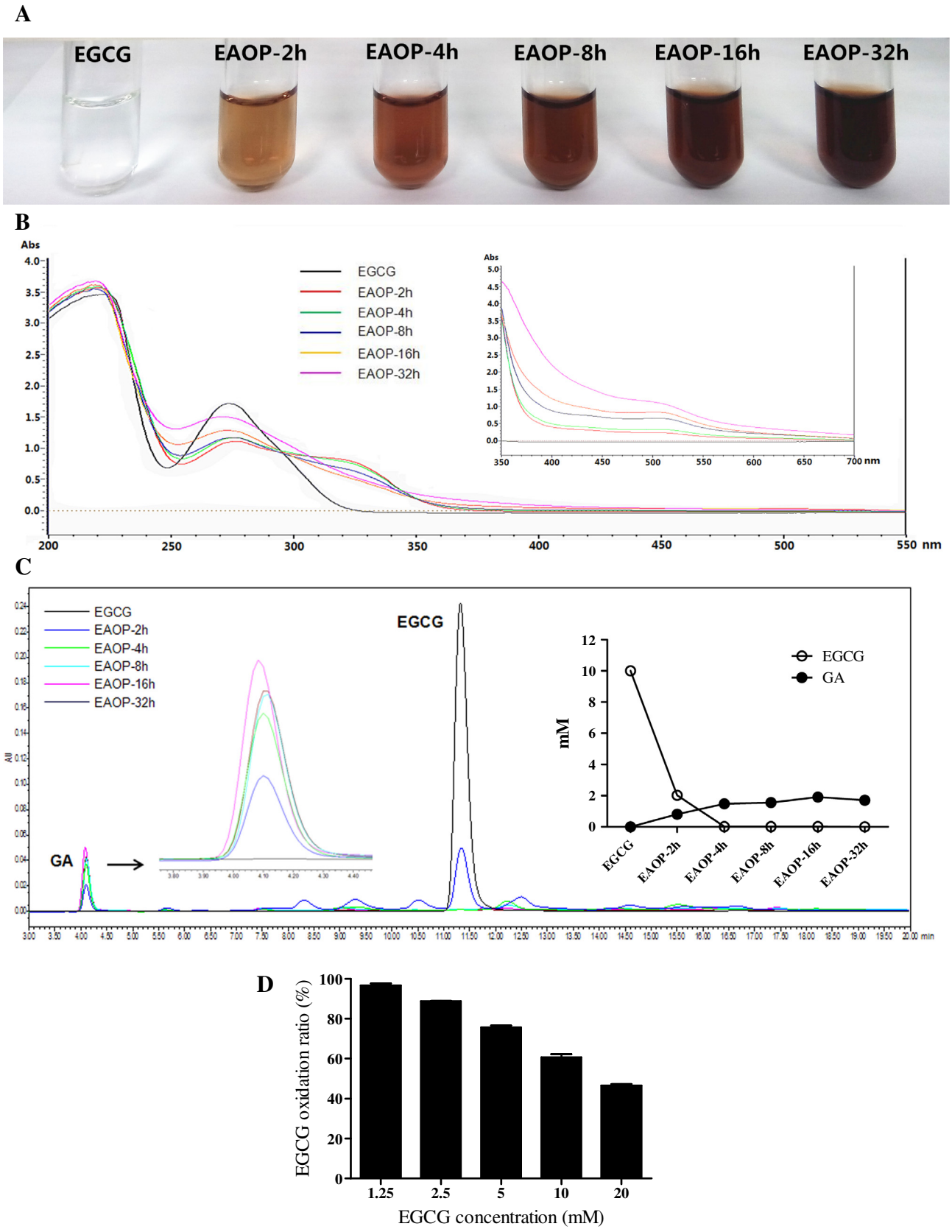

Fig. 1. Characterization of EAOPs. (A) Time-dependent color changes of EAOPs. (B) Time-dependent spectrum changes of EAOPs. (C) HPLC analysis of EGCG and GA content in native EGCG and EAOPs. (D) Oxidation ratio of different concentrations of EGCG after auto-oxidation for 1 h at 37 °C in 200 mM PBS (pH 8.0). Data are presented as mean ± SEM (n = 3 in C or 2 in D).

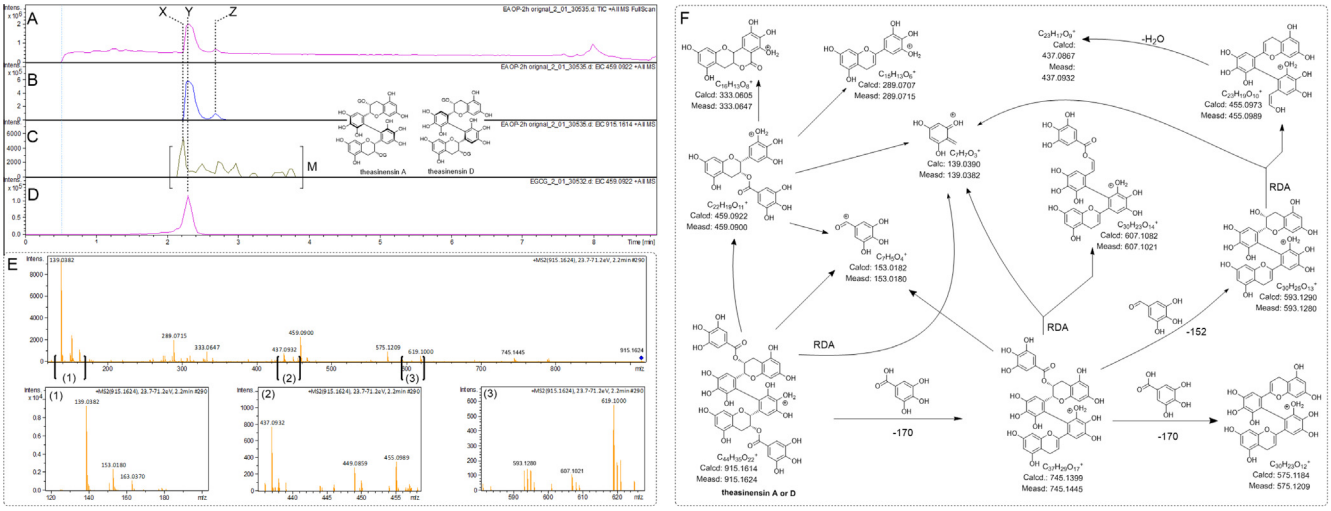

Fig. 2. Characterization of 2-h EAOPs. (A) TIC of 2-h EAOPs. (B) EIC of 459.0922 {calcd $[M + H]^+$ of EGCG (peak-Y) or GCG (peak-Z)} in 2-h EAOPs. (C) EIC of 915.1614 {calcd $[M + H]^+$ of theasinensin A or D}. The main chromatographic peak at 2.2 min (peak-X) was indicated as that of theasinensin A (or D) because among all the peaks with quasi molecular weight of 915.1614 (M), only peak-X showed clear fragmentation of [M-GA] and [M-2 × GA] in the MS/MS spectrum. (D) EIC of 459.0922 in EGCG standard. (E) The MS/MS spectrum of peak-X. (F) Possible MS/MS fission pathway of theasinensin A (or D).

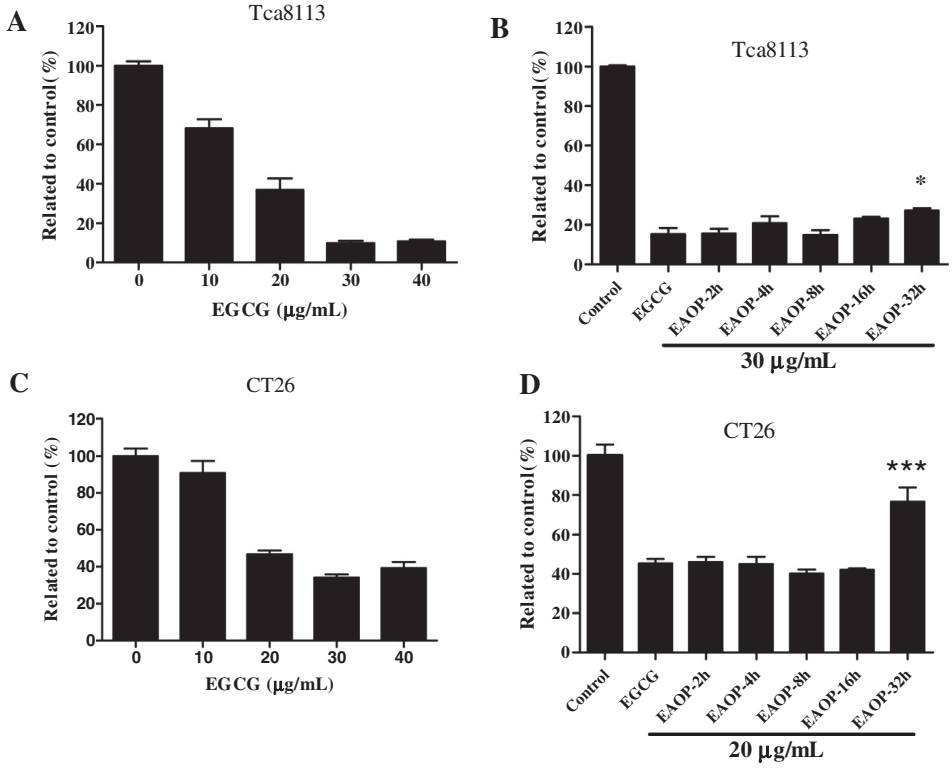

Fig. 3. Anti-proliferative activities of EGCG and EAOPs. (A) Dose effect of EGCG on Tca8113 proliferation. (B) Anti-proliferative effect of EGCG and EAOPs at the same concentration on Tca8113 cells. (C) Dose effect of EGCG on CT26 proliferation. (D) Anti-proliferative effect of EGCG and EAOPs at the same concentration on CT26 cells. Data are presented as mean ± SEM ($n = 6$). ∗ and ∗∗∗, $P < 0.05$ and $P < 0.001$, respectively, compared to EGCG.

and SOD abolished ROS production fully (Fig. 4E). However, ROS generated from 16-h EAOPs may contain other reactive oxygen species in addition to superoxide anions and hydrogen peroxide because the combination of CAT and SOD was unable to thoroughly scavenge ROS (Fig. 4F). It is worth noting that CAT appeared to be less effective in 16-h EAOPs than EGCG in terms of suppressing ROS (Fig. 4E, F). It can be speculated that the potential reason for this discrepancy is the reduced production of hydrogen peroxide in 16-h EAOPs compared to that in EGCG (Fig. 4B).

Mammalian TrxR1 is a selenocysteine-containing selenoenzyme, which is highly expressed in cancer cells and a putative target for cancer prevention and treatment. TrxR1 has a Cys/selenocysteine couple in the redox-active site within the C-terminal tetrapeptide motif. EGCG ortho-quinone, the key reactive group in EAOPs, readily reacts with the Cys/selenocysteine couple to form an irreversible conjugate, leading to inhibition of TrxR1 activity (Zhang et al., 2010). In the present study, EGCG was incubated with TrxR1 at pH 8.0 and 37 °C for 20 min in the presence of

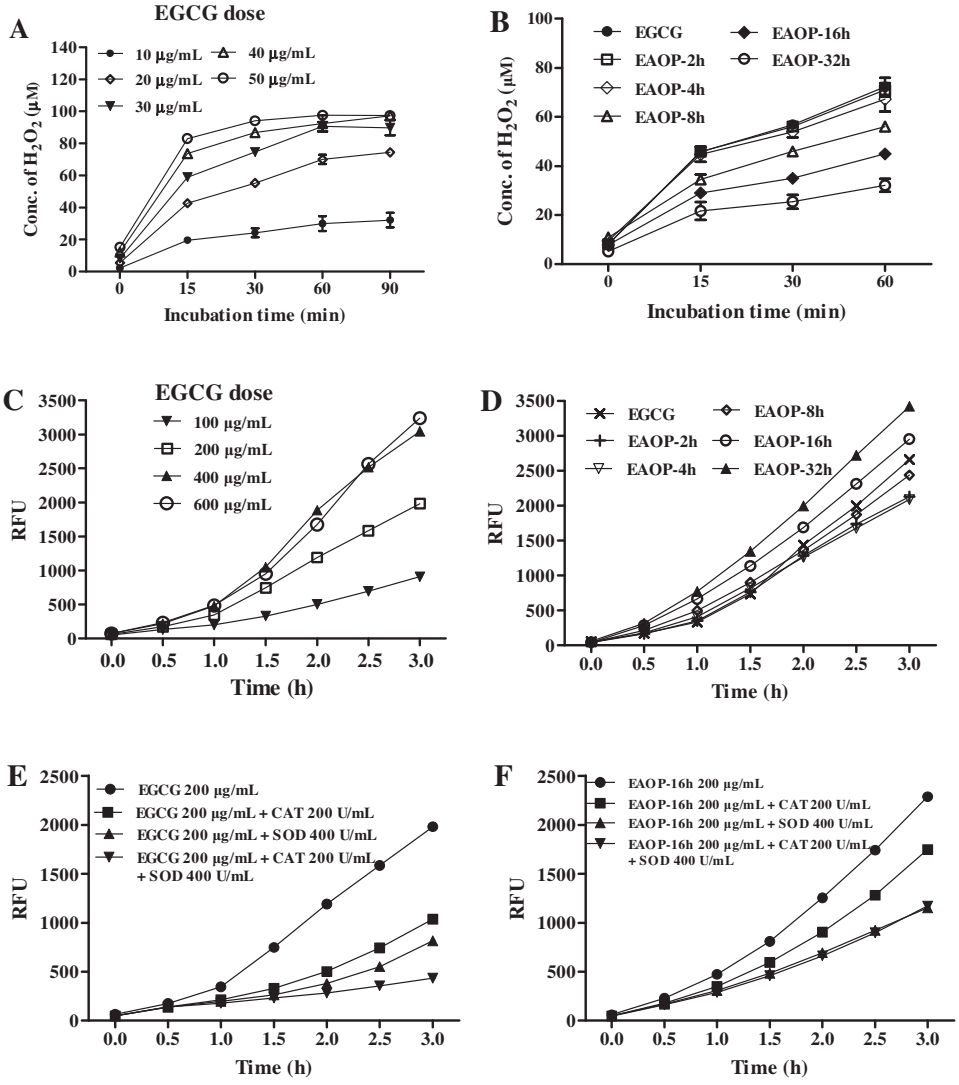

Fig. 4. Capacity of EGCG and EAOPs to produce hydrogen peroxide and ROS. (A) Dose effect of EGCG on hydrogen peroxide production. (B) Comparison of EGCG and EAOPs (20 μg/mL) generated hydrogen peroxide. (C) Dose effect of EGCG on ROS production. (D) Comparison of EGCG and EAOPs (200 μg/mL) generated ROS. (E) Effect of SOD and CAT on EGCG-generated ROS. (F) Effect of SOD and CAT on EAOPs-generated ROS. Data are presented as mean ± SEM (n = 2 or 3).

sufficient NADPH to allow maintenance of the Cys/selenocysteine couple in the fully reducing state. EGCG exhibited a dose-dependent inhibitory effect on TrxR1 activity (Fig. 5A), and we found that EGCG and EAOPs at a same concentration (5 μg/mL) had identical potency in the inhibition of TrxR1 activity (Fig. 5B).

However, all tested EAOPs irrespective of auto-oxidation time, were more robust than native EGCG in reacting with thiols in GSH and Cys (Fig. 6A and D). Both EGCG and 16-h EAOPs depleted GSH and Cys in a dose- (Fig. 6B and E) and time-dependent manner (Fig. 6C and F). Under any conditions, GSH or Cys depletion was more pronounced in 16-h EAOPs than in EGCG. Moreover, comparisons of Fig. 6A and D as well as Fig. 6C and F revealed that EAOPs reacted with Cys more efficiently than with GSH. Specifically, to achieve comparable thiol depletion by certain EAOPs required twice as long for GSH than for Cys. To observe whether the reaction of EAOP and Cys affects the cytotoxic activity of EAOP, 4-h EAOP (5 mg/mL) was incubated with the PBS as a control or 25 mM Cys at 37 °C for 3 h, and then their capacities of producing ROS and cytotoxic activities were evaluated. It was found that both the EAOP-Cys complexes and the EAOPs had a same ability to generate ROS (Fig. 6G); this may be an important reason why the cytotoxic activities of the EAOP-Cys did not compromised as compared with the EAOPs (Fig. 6H and I).

4. Discussion

EGCG has long been known as an antioxidant. Emerging evidence indicates that high-dose EGCG *in vivo* however triggers pro-oxidant effects. It has been reported that EGCG concentrations of mouse serum collected immediately and 4 h after intraperitoneal injection (*ip*) of 40 mg/kg EGCG were approximately 17 μM and undetectable, respectively (Siddiqui et al., 2009), thereby demonstrating that EGCG at a widely employed pharmacological dose is able to instantly increase blood drug concentrations comparable to those used in cell culture systems, and implying that serum EGCG undergoes rapid oxidation to trigger pro-oxidative responses. Being consistent with this concept, repeated EGCG treatments at a daily dose of 30 mg/kg (*ip*) that was needed for achieving a robust anti-cancer efficacy in mice markedly increased the levels of phosphorylated histone 2AX (γ-H2AX), a sensitive biomarker of oxidative stress, in tumor tissues

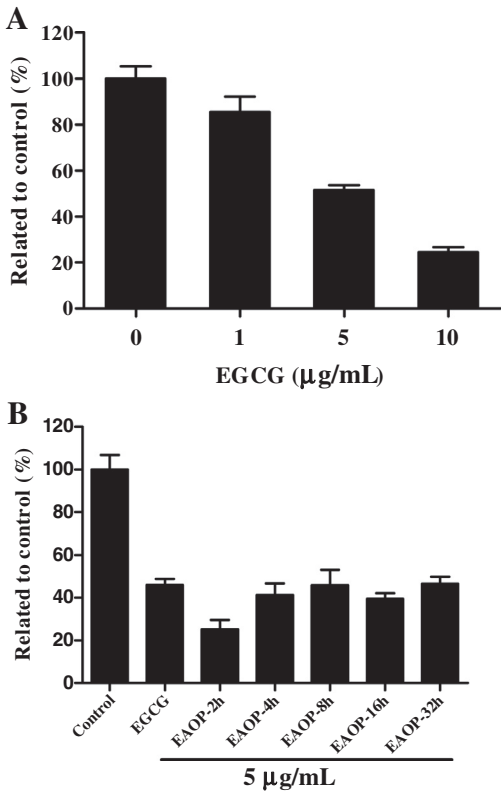

Fig. 5. Inhibitory effect of EGCG and EAOPs on TrxR1 activity. (A) Dose effect of EGCG. (B) Comparison of EGCG and EAOPs. Data are presented as mean ± SEM ($n = 3$).

(Li et al., 2010). Further more, a little bit elevation of EGCG dose (55 or 75 mg/kg, *ip*) resulted in pronounced increase of hepatic γ-H2AX levels and consequent hepatotoxicity in mice (Wang, Wang, Wan, Yang, & Zhang, 2015; Wang, Wei, et al., 2015). The pro-oxidative effect of EGCG in essence involves EGCG oxidation with the formations of ROS and EGCG oxidation products (Lambert & Elias, 2010). EGCG underwent rapid auto-oxidation in cell culture condition with a normal oxygen partial pressure of 160 mmHg. The auto-oxidation action could be significantly inhibited by SOD (Hong et al., 2002). *In vivo*, oxygen partial pressures in different tissues and circulating blood parts are not the same. Pulmonary alveolus and arterial blood have higher levels of oxygen partial pressure (⩾100 mm Hg), whereas it is below 40 mmHg in venous blood or other tissues (Sang, Lee, Hou, Ho, & Yang, 2005), therefore, auto-oxidation degree of EGCG *in vivo* should be attenuated compared with *in vitro* conditions due to reduced oxygen partial pressure, let alone the presence of SOD. However, many studies suggest that EGCG oxidation can be promoted by cytochrome P450 peroxidase activity, myeloperoxidase and tyrosinase (Dickerhof, Magon, Tyndall, Kettle, & Hampton, 2014; Ishii et al., 2008; Moridani, Scobie, Salehi, & O'Brien, 2001; Muzolf-Panek et al., 2008), oxidants released from neutrophils (Meotti et al., 2008) and endogenous copper (Hadi et al., 2007), likely including ceruloplasmin secreted from the liver with polyphenol oxidase activity (Floris, Medda, Padiglia, & Musci, 2000). Overall, the pro-oxidative property of EGCG or EGCG oxidation is influenced by its dose levels and exposed environments.

Biological activities of enzyme-catalyzed catechin oxidation products have been evaluated *in vitro* and *in vivo*. Catechin polymers formed in the presence of horseradish peroxidase had a higher antioxidant activity and xanthine oxidase inhibitory activity relative to catechin (Kurisawa, Chung, Kim, Uyama, & Kobayashi, 2003). Catechin polymers formed in the presence of laccase exhibited a better antihyperglycemic effect than catechin in mice (Jeon, Oh, Kim, & Imm, 2013) and gained an enhanced capacity of inhibiting pancreatic cholesterol esterase and cholesterol incorporation into micelles compared to catechin monomer (Jeon & Imm, 2014). Similarly, rutin polymers formed in the presence of laccase more effectively suppressed triglyceride accumulation than rutin monomer in 3T3-L1 adipocytes (Jeon, Lee, & Imm, 2014). Biological activities of EGCG oxidation products have not been characterized. EGCG oxidation involves many pathways including auto-oxidation, transition metal ion or oxidant-promoted oxidation and enzyme-catalyzed oxidation as demonstrated above. Whatever oxidation route, EGCG always undergoes polymerization, leading to the formation of numerous EGCG oxidation products (Lambert & Elias, 2010). To avoid separation of transition metal ions, oxidants or enzymes which otherwise would be a confounding factor affecting the interpretation of biological properties of EGCG oxidation products, we herein employed auto-oxidation pathway to prepare EAOPs. Although EAOPs did not exactly mirror EGCG oxidation products formed *in vivo*, the chemical and biological properties of EAOPs are helpful for in-depth understanding of extensively-documented cytotoxic action of EGCG *in vitro* and may help gain an insight into anti-cancer or toxicological mechanisms of EGCG *in vivo*.

The results of the present study show that EGCG is liable to undergo auto-oxidation and that the resultant EAOPs are also unstable. It has been reported that theasinensin A, an EGCG dimer, was formed as a transient intermediate along with EGCG auto-oxidation, whereas gallocatechin gallate (GCG), an epimer of EGCG, was formed when auto-oxidation speed of EGCG was protracted by SOD (Hong et al., 2002). In addition, EGCG quinone and EGCG dimer quinone have been identified during EGCG auto-oxidation (Sang et al., 2007). The current study showed that GCG and theasinensin A (or D) were present in 2-h EAOPs. Compared to native EGCG, the present study showed that extensive auto-oxidation of EGCG tended to compromise cytotoxic activities, but mild or moderate auto-oxidation of EGCG did not alter cytotoxic activities. The auto-oxidation action of EGCG also occurs under cell culture conditions. For example, the half-life of EGCG was less than 30 min in McCoy's 5A culture media (Hong et al., 2002); thus, it is reasonable to consider that EGCG and the resulting EAOPs work in concert to exert cytotoxic effects.

Cys levels in cancer cells can reach 100–150 μM, whereas GSH levels are below 20 μM (Chaiswing, Zhong, Liang, Jones, & Oberley, 2012; Olm et al., 2009); thus, Cys is the major component of extracellular thiols, and the extracellular reductive microenvironment is mainly dependent on the Cys/cystine pool but not on the GSH/GSSG pool (Moriarty-Craige & Jones, 2004). An extracellular redox state that is more reducing than a physiologic microenvironment redox state stimulates tumor progression and cancer cell invasion (Chaiswing et al., 2012; Venè et al., 2011). The reductive microenvironment is maintained by the Xc^- transporter that promotes cystine uptake. Intracellular cystine is then reduced to Cys for secretion into the extracellular environment (Lo, Wang, & Gout, 2008). Xc^- overexpression increases extracellular Cys levels and renders the cells resistant to oxidative stress (Banjac et al., 2008). Me-CA cells, which have an increased rate of Cys release, are resistant to As_2O_3 treatment (Venè et al., 2011). Therefore, compounds with the capacity to deplete extracellular Cys are likely to reduce cancer cell malignancy such as invasion and resistance to chemotherapeutic treatments. Several lines of evidence have demonstrated that Cys residues can be covalently conjugated by EGCG (Ishii et al., 2008). In fact, the covalent binding of EGCG and Cys residues involves EGCG auto-oxidation. Under neutral or alkaline pH conditions, EGCG auto-oxidation results in the formation of an EGCG ortho-quinone at the B- or the D-ring. These

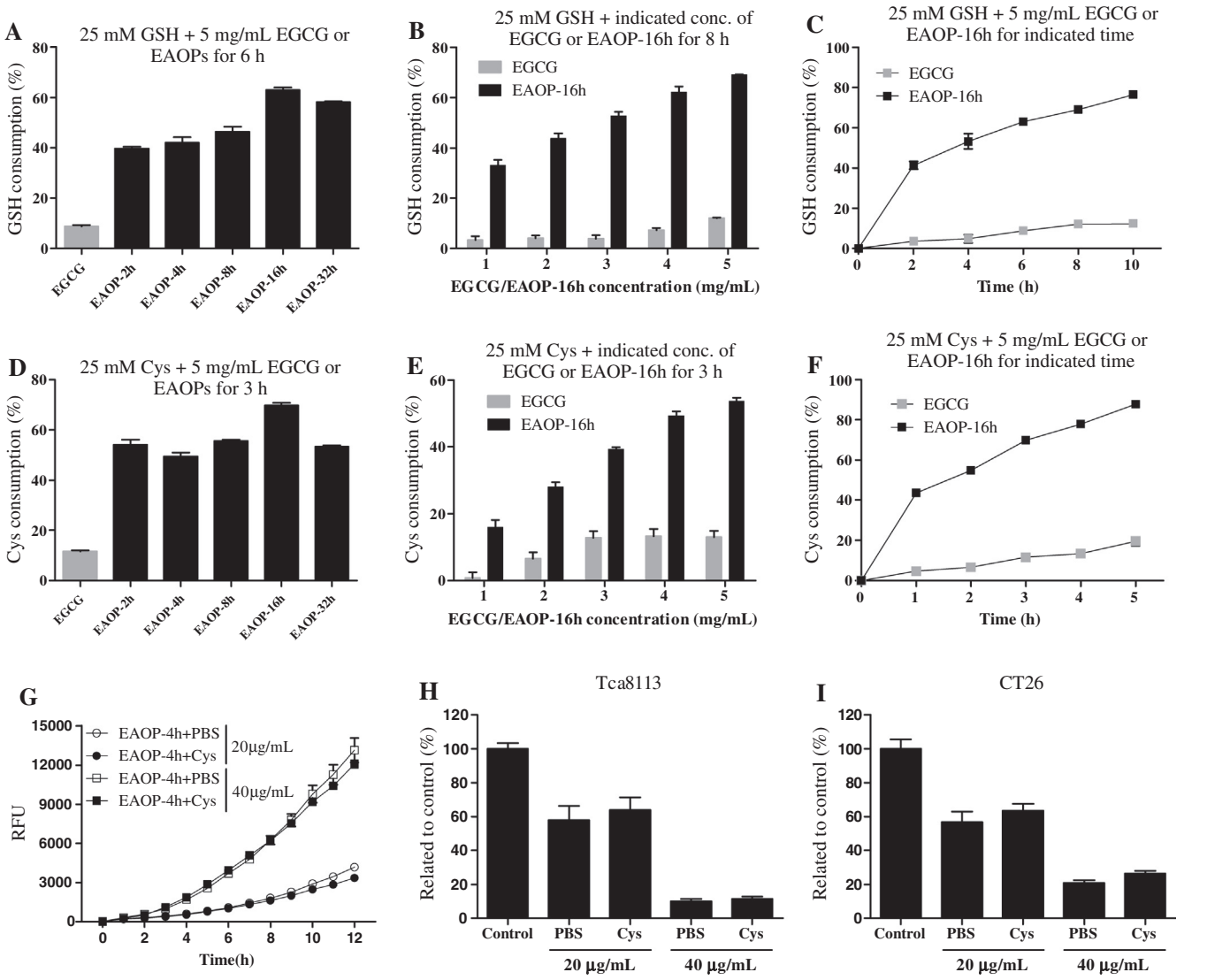

Fig. 6. Effect of EGCG and EAOPs on GSH and Cys. (A and D) Sulfhydryl group depletion of GSH or Cys. (B and E) Dose effect of EGCG and EAOPs on GSH or Cys. (C and F) Time effect of EGCG and EAOPs on GSH or Cys. (G) ROS production. (H and I) Anti-proliferative effect. Data are presented as mean ± SEM (n = 3 in A–G or 6 in H, I).

ortho-quinones result in the conjugation of sulfhydryl groups with EGCG (Muzolf-Panek et al., 2008; Sang et al., 2005). The present study revealed that: (1) EAOPs gained an enhanced ability to deplete Cys compared to native EGCG; (2) the sulfhydryl group of Cys was more efficiently depleted than that of GSH by EAOPs; (3) different EAOPs had an almost same capacity to react with the sulfhydryl group of Cys; (4) EAOP-Cys complexes still possessed comparable cytotoxic activity to EAOP; and (5) EAOPs presumably reacted with sulfhydryl group of GSH or Cys mainly via covalent conjugation according to following inferences: (a) EAOPs were derived from EGCG, suggesting that EAOPs, like EGCG dimer quinone, consisted of molecular skeleton of EGCG quinone, (b) all tested EAOPs at a concentration of 5 mg/mL that were equivalent to 10 mM EGCG depleted approximate 50% thiols of 25 mM GSH or Cys (Fig. 6A and D), such a nearly stoichiometric reaction implies the mechanism by which EAOPs decrease free thiols is principally attributed to covalent conjugation of sulfhydryl group with molecular skeleton of EGCG quinone. Based on these findings, it is tempting to consider that the reduced malignancy of cancer cells subjected to EGCG treatments (Kato et al., 2008; Lim et al., 2008) also involve the influence of extracellularly formed EGCG oxidation products on extracellular Cys.

5. Conclusions

EGCG is liable to undergo auto-oxidation to form diverse EAOPs. Compared to native EGCG, EAOPs gained an enhanced capacity to deplete sulfhydryl group of cysteine which is a major extracellular constitute responsible for sustaining cancer cell malignancy. Certain EAOPs that no longer contain EGCG retains the capacities of EGCG to produce ROS including hydrogen peroxide and inhibit thioredoxin reductase, which is a putative target for cancer prevention and treatment. Auto-oxidation action of EGCG does not necessarily compromise its cytotoxic effects. The anti-cancer activity of EGCG involves a joint contribution of EGCG and vast numbers of bioactive EGCG oxidation products formed extracellularly.

Conflict of interest

The authors have no conflict of interest to declare.

Acknowledgements

We thank Prof. Pieter C. Dorrestein and Dr. Alexey Melnik, Skaggs School of Pharmacy and Pharmaceutical Sciences, Univer-

sity of California, San Diego, for supplying the UPLC–ESI-MS instrument, and assistance in dereplication of some MS/MS data. This work was supported by National Natural Science Foundation of China (31170648, 31471720), Anhui Major Demonstration Project for Leading Talent Team on Tea Chemistry and Health, Funds of Anhui Provincial Science and Technology Department (1306c083018), Funds of Anhui Provincial Education Department (2013SQRL119ZD), Collaborative Innovation Center of Agri-forestry Industry in Dabieshan Area, Tea Project of Anhui Provincial Agriculture Committee, Anhui Agricultural University, and Foundation of AHAU Subject Construction (XKTS2013017).

Appendix A. Supplementary data

Supplementary data associated with this article can be found, in the online version, at http://dx.doi.org/10.1016/j.foodchem.2016.02.134.

References

Banjac, A., Perisic, T., Sato, H., Seiler, A., Bannai, S., Weiss, N., et al. (2008). The cystine/cysteine cycle: A redox cycle regulating susceptibility versus resistance to cell death. *Oncogene, 27*, 1618–1628.

Chaiswing, L., Zhong, W., Liang, Y., Jones, D. P., & Oberley, T. D. (2012). Regulation of prostate cancer cell invasion by modulation of extra- and intracellular redox balance. *Free Radical Biology and Medicine, 52*, 452–461.

Dickerhof, N., Magon, N. J., Tyndall, J. D., Kettle, A. J., & Hampton, M. B. (2014). Potent inhibition of macrophage migration inhibitory factor (MIF) by myeloperoxidase-dependent oxidation of epicatechins. *The Biochemical Journal, 462*, 303–314.

Floris, G., Medda, R., Padiglia, A., & Musci, G. (2000). The physiopathological significance of ceruloplasmin. A possible therapeutic approach. *Biochemical Pharmacology, 60*, 1735–1741.

Hadi, S. M., Bhat, S. H., Azmi, A. S., Hanif, S., Shamim, U., & Ullah, M. F. (2007). Oxidative breakage of cellular DNA by plant polyphenols: A putative mechanism for anticancer properties. *Seminars in Cancer Biology, 17*, 370–376.

Hong, J., Lu, H., Meng, X., Ryu, J. H., Hara, Y., & Yang, C. S. (2002). Stability, cellular uptake, biotransformation, and efflux of tea polyphenol (−)-epigallocatechin-3-gallate in HT-29 human colon adenocarcinoma cells. *Cancer Research, 62*, 7241–7246.

Ishii, T., Mori, T., Tanaka, T., Mizuno, D., Yamaji, R., Kumazawa, S., et al. (2008). Covalent modification of proteins by green tea polyphenol (−)-epigallocatechin-3-gallate through autoxidation. *Free Radical Biology and Medicine, 45*, 1384–1394.

Jeon, S. Y., & Imm, J. Y. (2014). Lipase inhibition and cholesterol-lowering activities of laccase-catalyzed catechin polymers. *Food Science and Biotechnology, 23*, 1703–1707.

Jeon, J. K., Lee, J., & Imm, J. Y. (2014). Effects of laccase-catalyzed rutin polymer fraction on adipogenesis inhibition in 3T3-L1 adipocytes. *Process Biochemistry, 49*, 1189–1195.

Jeon, S. Y., Oh, S., Kim, E., & Imm, J. Y. (2013). α-Glucosidase inhibiton and antiglycation activity of laccase-catalyzed catechin polymers. *Journal of Agricultural and Food Chemistry, 61*, 4577–4584.

Kato, K., Long, N. K., Makita, H., Toida, M., Yamashita, T., Hatakeyama, D., et al. (2008). Effects of green tea polyphenol on methylation status of RECK gene and cancer cell invasion in oral squamous cell carcinoma cells. *British Journal of Cancer, 99*, 647–654.

Khan, N., & Mukhtar, H. (2013). Tea and health: Studies in humans. *Current Pharmaceutical Design, 19*, 6141–6147.

Kumazoe, M., Sugihara, K., Tsukamoto, S., Huang, Y., Tsurudome, Y., Suzuki, T., et al. (2013). 67-kDa laminin receptor increases cGMP to induce cancer-selective apoptosis. *The Journal of Clinical Investigation, 123*, 787–799.

Kurisawa, M., Chung, J. E., Kim, Y. J., Uyama, H., & Kobayashi, S. (2003). Amplification of antioxidant activity and xanthine oxidase inhibition of catechin by enzymatic polymerization. *Biomacromolecules, 4*, 469–471.

Lambert, J. D., & Elias, R. J. (2010). The antioxidant and pro-oxidant activities of green tea polyphenols: A role in cancer prevention. *Archives of Biochemistry and Biophysics, 501*, 65–72.

Li, G. X., Chen, Y. K., Hou, Z., Xiao, H., Jin, H., Lu, G., et al. (2010). Pro-oxidative activities and dose-response relationship of (−)-epigallocatechin-3-gallate in the inhibition of lung cancer cell growth: A comparative study in vivo and in vitro. *Carcinogenesis, 31*, 902–910.

Lim, Y. C., Park, H. Y., Hwang, H. S., Kang, S. U., Pyun, J. H., Lee, M. H., et al. (2008). (−)-Epigallocatechin-3-gallate (EGCG) inhibits HGF-induced invasion and metastasis in hypopharyngeal carcinoma cells. *Cancer Letters, 271*, 140–152.

Lo, M., Wang, Y. Z., & Gout, P. W. (2008). The x(c)-cystine/glutamate antiporter: A potential target for therapy of cancer and other diseases. *Journal of Cellular Physiology, 215*, 593–602.

Menet, M. C., Sang, S. M., Yang, C. S., Ho, C. T., & Rosen, R. T. (2004). Analysis of theaflavins and thearubigins from black tea extract by Maldi-Tof mass spectrometry. *Journal of Agricultural and Food Chemistry, 52*, 2455–2461.

Meotti, F. C., Senthilmohan, R., Harwood, D. T., Missau, F. C., Pizzolatti, M. G., & Kettle, A. J. (2008). Myricitrin as a substrate and inhibitor of myeloperoxidase: Implications for the pharmacological effects of flavonoids. *Free Radical Biology and Medicine, 44*, 109–120.

Moriarty-Craige, S. E., & Jones, D. P. (2004). Extracellular thiols and thiol/disulfide redox in metabolism. *Annual Review of Nutrition, 24*, 481–509.

Moridani, M. Y., Scobie, H., Salehi, P., & O'Brien, P. J. (2001). Catechin metabolism: Glutathione conjugate formation catalyzed by tyrosinase, peroxidase, and cytochrome p450. *Chemical Research in Toxicology, 14*, 841–848.

Muzolf-Panek, M., Gliszczyńska-Swigło, A., de Haan, L., Aarts, J. M., Szymusiak, H., Vervoort, J. M., et al. (2008). Role of catechin quinones in the induction of EpRE-mediated gene expression. *Chemical Research in Toxicology, 21*, 2352–2360.

Olm, E., Fernandes, A. P., Hebert, C., Rundlöf, A. K., Larsen, E. H., Danielsson, O., et al. (2009). Extracellular thiol-assisted selenium uptake dependent on the x(c)-cystine transporter explains the cancer-specific cytotoxicity of selenite. *Proceedings of the National Academy of Sciences of the United States of America, 106*, 11400–11405.

Sang, S., Lambert, J. D., Ho, C. T., & Yang, C. S. (2011). The chemistry and biotransformation of tea constituents. *Pharmacological Research, 64*, 87–99.

Sang, S., Lambert, J. D., Hong, J., Tian, S., Lee, M. J., Stark, R. E., et al. (2005). Synthesis and structure identification of thiol conjugates of (−)-epigallocatechin gallate and their urinary levels in mice. *Chemical Research in Toxicology, 18*, 1762–1769.

Sang, S., Lee, M. J., Hou, Z., Ho, C. T., & Yang, C. S. (2005). Stability of tea polyphenol (−)-epigallocatechin-3-gallate and formation of dimers and epimers under common experimental conditions. *Journal of Agricultural and Food Chemistry, 53*, 9478–9484.

Sang, S., Yang, I., Buckley, B., Ho, C. T., & Yang, C. S. (2007). Autoxidative quinone formation in vitro and metabolite formation in vivo from tea polyphenol (−)-epigallocatechin-3-gallate: Studied by real-time mass spectrometry combined with tandem mass ion mapping. *Free Radical Biology and Medicine, 43*, 362–371.

Severino, J. F., Goodman, B. A., Kay, C. W., Stolze, K., Tunega, D., Reichenauer, T. G., et al. (2009). Free radicals generated during oxidation of green tea polyphenols: Electron paramagnetic resonance spectroscopy combined with density functional theory calculations. *Free Radical Biology and Medicine, 46*, 1076–1088.

Shammas, M. A., Neri, P., Koley, H., Batchu, R. B., Bertheau, R. C., Munshi, V., et al. (2006). Specific killing of multiple myeloma cells by (−)-epigallocatechin-3-gallate extracted from green tea: Biologic activity and therapeutic implications. *Blood, 108*, 2804–2810.

Siddiqui, I. A., Adhami, V. M., Bharali, D. J., Hafeez, B. B., Asim, M., Khwaja, S. I., et al. (2009). Introducing nanochemoprevention as a novel approach for cancer control: Proof of principle with green tea polyphenol epigallocatechin-3-gallate. *Cancer Research, 69*, 1712–1716.

Venè, R., Castellani, P., Delfino, L., Lucibello, M., Ciriolo, M. R., & Rubartelli, A. (2011). The cystine/cysteine cycle and GSH are independent and crucial antioxidant systems in malignant melanoma cells and represent druggable targets. *Antioxidants and Redox Signaling, 15*, 2439–2453.

Wang, X., Sun, K., Tan, Y., Wu, S., & Zhang, J. (2014). Efficacy and safety of selenium nanoparticles administered intraperitoneally for the prevention of growth of cancer cells in the peritoneal cavity. *Free Radical Biology and Medicine, 72*, 1–10.

Wang, D., Taylor, E. W., Wang, Y., Wan, X., & Zhang, J. (2012). Encapsulated nanoepigallocatechin-3-gallate and elemental selenium nanoparticles as paradigms for nanochemoprevention. *International Journal of Nanomedicine, 7*, 1711–1721.

Wang, D., Wang, Y., Wan, X., Yang, C. S., & Zhang, J. (2015). Green tea polyphenol (−)-epigallocatechin-3-gallate triggered hepatotoxicity in mice: Responses of major antioxidant enzymes and the Nrf2 rescue pathway. *Toxicology and Applied Pharmacology, 283*, 65–74.

Wang, D., Wei, Y., Wang, T., Wan, X., Yang, C. S., Reiter, R. J., et al. (2015). Melatonin attenuates (−)-epigallocatehin-3-gallate-triggered hepatotoxicity without compromising its downregulation of hepatic gluconeogenic and lipogenic genes in mice. *Journal of Pineal Research, 59*, 497–507.

Yang, C. S., & Hong, J. (2013). Prevention of chronic diseases by tea: Possible mechanisms and human relevance. *Annual Review of Nutrition, 33*, 161–181.

Yuan, J. M. (2013). Cancer prevention by green tea: Evidence from epidemiologic studies. *The American Journal of Clinical Nutrition, 98*, S1676–S1681.

Zhang, H., Cao, D., Cui, W., Ji, M., Qian, X., & Zhong, L. (2010). Molecular bases of thioredoxin and thioredoxin reductase-mediated prooxidant actions of (−)-epigallocatechin-3-gallate. *Free Radical Biology and Medicine, 49*, 2010–2018.

Zhang, L., Wei, Y., & Zhang, J. (2014). Novel mechanisms of anticancer activities of green tea component epigallocatechin- 3-gallate. *Anti-cancer Agents in Medicinal Chemistry, 14*, 779–786.